Sample No.	Date of sample collection	Sampling site	Water volume	Microscopic observation (number of oocysts)	Original RT-LAMP*1	Improved RT-LAMP*2
41		OTS	10l	0	−	−
42		ONP	10l	0	−	−
43	29Oct.2009	TK	10l	0	−	−
44	04Nov.2009	HIK	10l	0	−	−
45		HIM	10l	0	−	−
46	10Nov.2009	OHK	10l	0	−	−
47		OHM	10l	0	−	−
48		OOG	10l	0	−	−
49		IKN	10l	1	−	+
50	09Feb.2010	IKN	10l	0	−	+
Number of total samples (including divided samples)				44 (50)		
Number of positive samples (including divided samples)				4 (4)	9 (10)	11 (12)
Positive rate (including divided samples) (%)				9.1 (8.0)	20.5 (20.0)	25.0 (24.0)

*1 Original RT-LAMP assay was performed using 5μl of *Cryptosporidium* RNA extract.
*2 Improved RT-LAMP assay was performed using 1μl of *Cryptosporidium* RNA extract.
*3 + : positive
*4 − : negative

れた試料に比べると、表流水の汚染は大きく希釈されており、阻害物質の存在量が少ないことから、改善効果が少なくなったものと考えられた。しかし、RT-LAMP改善法によって表流水中の阻害物質の影響が緩和されたことは変わりない。No.20の試料のみ、RT-LAMP従来法で陽性であったのがRT-LAMP改善法で陰性となった。この試料は検鏡法でクリプトスポリジウムが不検出であり、存在するオーシスト数が極めて少ない、あるいは存在するオーシストが壊れる途中で核酸が不安定であったと考えられた。

湧水（9検体）、浅井戸水（4検体）、伏流水（1検体）、浄水（13検体）からは、いずれの方法によってもクリプトスポリジウムは検出されなかった（Table 4）。これらの検体はクリプトスポリジウム汚染がほとんどないと考えられることから、RT-LAMP反応に偽陽性は生じていないと考えられた。

RT-LAMP法で陽性となった増幅産物のアガロースゲル電気泳動を行い、増幅産物が*Cryptosporidium parvum*と同一のバンドパターンであることを確認した。泳動結果の一部をFig. 1（RT-LAMP従来法）及びFig.2（RT-LAMP改善法）に示した。

以上より、一連の増幅結果に偽陽性はなかったと判断した。RT-LAMP改善法は養豚場排水放流水だけでなく、環境水全般についてRT-LAMP従来法よりも検出感度が高く、これまでの検討では偽陽性も認められなかった。本法は検査に使用するRNA抽出液量を減らすだけで阻害が回避できる非常に簡便な改善法であり、検鏡法の結果との対比も得られていることから、RT-LAMP改善法の実用性は十分にあると判断した。本研究に用いた環境水及び検討した核酸抽出方法は限られていることから、検査対象水の阻害物質濃度とクリプトスポリジウム濃度、用いる核酸抽出方法が変われば、最適な核酸抽出液量は変化するものと考えられる。本研究で示した検鏡法との比較のみならず、さらなる核酸抽出法の最適化と、異なる配列を標的とした複数の遺伝子解析法を併用することにより、遺伝子検査法の信頼性の向上が図れると考えられる。顕微鏡による形態観察と遺伝子増幅による標的配列の検出とは原理が異なることから、必ずしも1：1対応はしないものの、遺伝子検査法はクリプトスポリジウム汚染の有無を明らかにする試験目的には十分に有用であると考えられた。今後、多くの検査機関においてRT-LAMP改善法を実施し、評価されることを望む。

4. まとめ

検水中の遺伝子増幅阻害物質の影響を除去するために、RT-LAMP反応に用いるRNA抽出液量を従来の5μlから1μlに低減した改善法を検討し、以下の知見を得た。

1）RT-LAMPの検出感度は6×10^{-3}オーシスト相当/RT-

Table 4 Detection results for *Cryptosporidium* oocysts in finished water, spring water, shallow well water and river-bed water by conventional microscopic observation, original RT-LAMP and improved RT-LAMP

Sample No.	Date of sample collection	Sampling site	Water type	Water volume	Microscopic observation (number of oocysts)	Original RT-LAMP[*1]	Improved RT-LAMP[*2]
1	01Dic.2008	YRS	FW[*3]	20*l*	0	−[*7]	−
2	24Feb.2009	HBT	FW	20*l*	0	−	−
3		OKD	FW	20*l*	0	−	−
4		SEY	FW	20*l*	0	−	−
5	23Aug.2009	HBT	FW	20*l*	0	−	−
6		OKD	FW	20*l*	0	−	−
7		SEY	FW	20*l*	0	−	−
8	01Dic.2009	OKD	FW	20*l*	0	−	−
9		SEY	FW	20*l*	0	−	−
10		YMZ	FW	20*l*	0	−	−
11	09Feb.2010	HBT	FW	20*l*	0	−	−
12		OKD	FW	20*l*	0	−	−
13		SEY	FW	20*l*	0	−	−
14	15Oct.2008	BRW	SP[*4]	10*l*	0	−	−
15		SNT	SP	10*l*	0	−	−
16		OGG	SP	10*l*	0	−	−
17	22Oct.2008	SND	SP	10*l*	0	−	−
18	14Oct.2009	SNT	SP	10*l*	0	−	−
19		NKN	SP	10*l*	0	−	−
20		BRW	SP	10*l*	0	−	−
21	15Oct.2009	OGG	SP	10*l*	0	−	−
22	21 Oct.2009	SND	SP	10*l*	0	−	−
23	09Dic.2008	OH1	SW[*5]	10*l*	0	−	−
24		OH2	SW	10*l*	0	−	−
25	24Feb.2009	OH1	SW	10*l*	0	−	−
26		OH2	SW	10*l*	0	−	−
27	01Dic.2008	AMZ	RB[*6]	10*l*	0	−	−
Number of total samples				27			
Number of positive samples				0	0	0	
Positive rate (%)				0	0	0	

[*1] Original RT-LAMP assay was performed using 5μl of *Cryptosporidium* RNA extract.
[*2] Improved RT-LAMP assay was performed using 1μl of *Cryptosporidium* RNA extract.
[*3] FW : Finished water
[*4] SP : Spring water
[*5] SW : Shallow well water
[*6] RB : River-bed water
[*7] − : negative

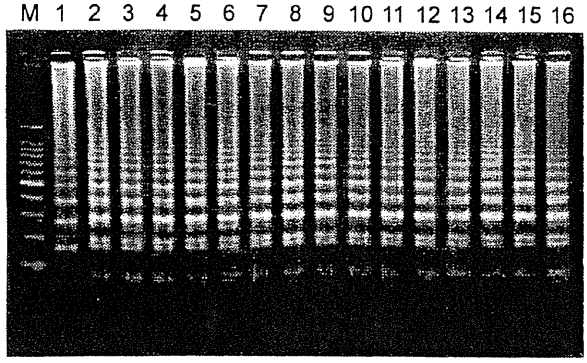

Fig. 1 Analysis of original RT-LAMP products of positive samples by agarose gel electrophoresis.

M : 100bp DNA ladder
1 : Positive control for LAMP reaction[a]
2 : Positive control for electrophoresis[b]
3 : Table 3 Sample No.1
4 : Table 3 Sample No. 2
5 : Table 3 Sample No.19
6 : Table 3 Sample No.20
7 : Table 3 Sample No.21
8 : Table 3 Sample No.22
9 : Table 3 Sample No.23
10 : Table 3 Sample No.24
11 : Table 2 Sample No.6
12 : Table 2 Sample No.7
13 : Table 2 Sample No.8
14 : Table 2 Sample No.9
15 : Table 2 Sample No.10
16 : Table 2 Sample No.11

[a]Positive control for the RT-LAMP assay made of RNA with an artificial sequence. The electrophoretic pattern of this positive control was different from that of *Cryptosporidium parvum* oocysts. If the electrophoretic pattern of samples was the same as lane 1, it was an evidence of contamination by the positive control.
[b]Positive control for electrophoresis which derives from nucleic acid of *Cryptosporidium parvum* oocysts. This positive control was not used in LAMP reactions.

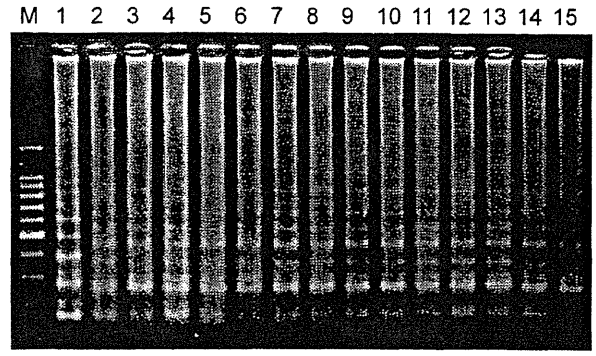

Fig. 2 Analysis of improved RT-LAMP products of positive samples by agarose gel electrophoresis.

M : 100bp DNA ladder
1 : Positive control for LAMP reaction[a]
2 : Positive control for electrophoresis[b]
3 : Table 2 Sample No.1
4 : Table 2 Sample No.2
5 : Table 2 Sample No.3
6 : Table 2 Sample No.9
7 : Table 2 Sample No.10
8 : Table 2 Sample No.11
9 : Table 2 Sample No.12
10 : Table 2 Sample No.17
11 : Table 2 Sample No.22
12 : Table 3 Sample No.19
13 : Table 3 Sample No.29
14 : Table 3 Sample No.39
15 : Table 3 Sample No.50

[a]Positive control for the RT-LAMP assay made of RNA with an artificial sequence. The electrophoretic pattern of this positive control was different from that of *Cryptosporidium parvum* oocysts. If the electrophoretic pattern of samples was the same as lane 1, it was an evidence of contamination by the positive control
[b]Positive control for electrophoresis which derives from nucleic acid of *Cryptosporidium parvum* oocysts. This positive control was not used in LAMP reactions.

LAMP反応であった。この検出感度から、RNA抽出液20 μl中の鋳型RNA液1 μlで1オーシストが検出可能と判断した（1オーシスト/20μl = 5 $\times 10^{-2}$オーシスト相当/1 μl）。

2）RT-LAMP改善法は、検査した養豚場排水放流水、その下流の河川水、その他の表流水全てにおいて、RT-LAMP従来法よりも高感度であり、偽陽性も認められなかった。養豚場排水放流水やその下流の河川水のように阻害が強いと考えられる検体では、検体を複数に分割し、それぞれの試料についてRT-LAMP改善法を実施することで、陽性率を高めることが可能であった。

謝 辞

本研究は平成19～21年度の厚生労働省科学研究費補助金「健康安全・危機管理対策総合研究事業　飲料水の水質リスク管理に関する統合的研究」（H19-健危-一般-012）の補助を受けて実施した。

参考文献

1）金子光美：水道の病原微生物対策，丸善，東京（2006）
2）Guillot, E. and Loret, J. F. : Cryptosporidium. Waterborne pathogens: Review for the drinking water industry, IWA Publishing, London UK (2010)
3）Yoder, J. S., Harral, C., and Beach, M. J. :

Cryptosporidiosis surveillance -- United Sates, 2006 -- 2008, MMRW, Vol.59, No.SS-6 (2010)
4) Smith, A., Reacher, M., Smerdon, W., Adak, G. K., Nichols, G., and Chalmers, R. M. : Review article: Outbreaks of water borne infectious intestinal disease in England and Wales, 1992-2003, Epidemiol. Infect., Vol.134, 1141-1149 (2006)
5) 埼玉県衛生部 :クリプトスポリジウムによる集団下痢症—越生町集団下痢症発生事件—報告書 (1997)
6) 厚生労働省健康局水道課長通知：水道における指標菌及びクリプトスポリジウム等の検査方法について 平成19年3月30日付健水発第0330006号 (2007)
7) Smith, H.V. and Nichols, R.A. : *Cryptosporidium*: detection in water and food, Exp Parasitol. , Vol. 124 (1), 61-79 (2010)
8) Inomata, A., Kishida, N., Momoda, T., Akiba, M., Izumiyama, S., Yagita, K., and Endo, T. : Development and evaluation of a reverse transcription-loop-mediated isothermal amplification assay for rapid and high-sensitive detection of *Cryptosporidium* in water samples, Water Sci. Technol., Vol.60, 2167-2172 (2009)
9) Lantz, P.G., Matsson, M., Wadstrom, T., and Radstrom, P. : Removal of PCR inhibitors from human faecal samples through the use of an aqueous two-phase system for sample preparation prior to PCR, Journal of Microbiological Methods, Vol. 28, 159-167 (1997)
10) Lund, M., Nordentoft, S., Pedersen, K., and Madsen, M. : Detection of *Campylobacter* spp. in chicken fecal samples by real-time PCR, Journal of Clinical Microbiology, Vol. 42, 5125-5132 (2004)
11) Kreader, C. A.: Relief of amplification inhibition in PCR with bovine serum albumin or T4 gene 32 protein, Applied and Environmental Microbiology, Vol. 62, 1102-1106 (1996)
12) 百田隆祥，小島禎，池戸正成，泉山信司，遠藤卓郎: LAMP法（Loop-Mediated Isothermal Amplification）を用いたクリプトスポリジウム及びジアルジアの高感度迅速検出，水環境学会誌. Vol.32, 321-324 (2009)
13) Yagita, K., Izumiyama, S., Tachibana, H., Masuda, G., Iseki, M., Furuya, K., Kameoka, Y., Kuroki, T., Itagaki, T., and Endo, T. : Molecular characterization of *Cryptosporidium* isolates obtained from human and bovine infections in Japan, Parasitology Research. Vol.87, 950-955 (2001)

(受付 2010.8.23)
(受理 2010.11.22)

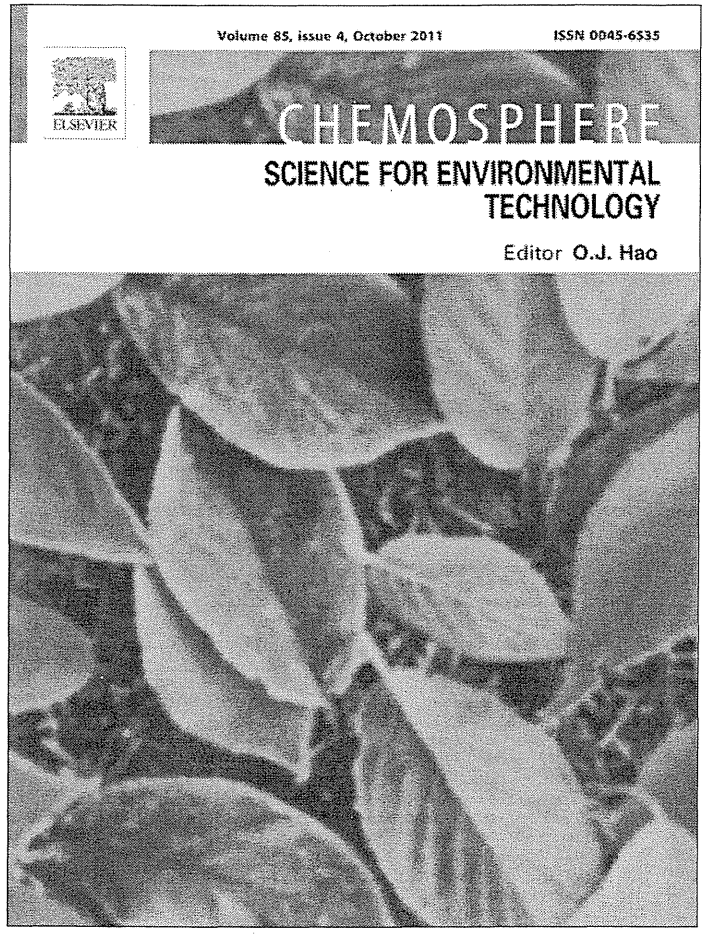

Chemosphere 85 (2011) 571–576

Contents lists available at ScienceDirect

Chemosphere

journal homepage: www.elsevier.com/locate/chemosphere

Virus inactivation during coagulation with aluminum coagulants

Taku Matsushita *, Nobutaka Shirasaki, Yoshihiko Matsui, Koichi Ohno

Graduate School of Engineering, Hokkaido University, N13W8, Sapporo 060-8628, Japan

ARTICLE INFO

Article history:
Received 24 March 2011
Received in revised form 21 June 2011
Accepted 21 June 2011
Available online 13 July 2011

Keywords:
Bacteriophage
Inactivation
Virus
Aluminum coagulant
Coagulation process

ABSTRACT

We used the bacteriophages Qβ and MS2 to determine whether viruses are inactivated by aluminum coagulants during the coagulation process. We performed batch coagulation and filtration experiments with virus-containing solutions. After filtering the supernatant of the coagulated solution through a membrane with a pore size of 50 nm, we measured the virus concentration by both the plaque forming unit (PFU) and polymerase chain reaction (PCR) methods. The virus concentration determined by the PFU method, which determines the infectious virus concentration, was always lower than that determined by the PCR-based method, which determines total virus concentration, regardless of infectivity. This discrepancy can be explained by the formation of aggregates consisting of several virus particles or by the inactivation of viruses in the coagulation process. The former possibility can be discounted because (i) aggregates of several virus particles would not pass through the 50-nm pores of the filtration membrane, and (ii) our particle size measurements revealed that the virus particles in the membrane filtrate were monodispersed. These observations clearly showed that non-infectious Qβ particles were present in the membrane filtrate after the coagulation process with aluminum coagulants. We subsequently revealed that the viruses lost their infectivity after being mixed with hydrolyzing aluminum species during the coagulation process.

1. Introduction

Advances in molecular biology have enabled the detection of viruses at low concentrations in environmental waters without the need for virus cultivation. By using these technologies, viruses have been detected in river water, drinking water sources, and in drinking water worldwide. These findings have highlighted the need for treating drinking water to remove viruses. The United States Environmental Protection Agency has included four waterborne viruses on Contaminant Candidate List 3 for drinking water (USEPA); these viruses are currently not subjected to drinking water regulations in the United States but are listed because they require regulation in the future.

Viruses can be removed from drinking water by different treatments, including virus inactivation and physicochemical separation processes. Virus inactivation treatment includes chlorination, ozonation, and UV light irradiation. In these processes, chlorine; an oxidant (ozone), as well as some radicals; and UV light penetrate the virion and reversibly or irreversibly modify the viral genome (Dennis et al., 1979; Camel and Bermond, 1998; Hijnen et al., 2006). The oxidants can also modify the surface protein of the virus (Camel and Bermond, 1998). Modification of the genome or surface protein of the virus abolishes the virus's infectivity. By comparison, in physicochemical separation processes, waterborne virus particles settle out under natural gravity after becoming enmeshed in aluminum/ferric flocs generated during the coagulation process. Alternatively, virus particles are filtered out by ultrafiltration, nanofiltration, or reverse osmosis membranes. In these treatments, viruses are physicochemically separated from the water.

Recently, our group found that the plaque forming unit (PFU)-based concentrations of viruses that had become enmeshed in aluminum floc did not recover to their initial values before coagulation, even after the floc was dissolved under alkaline conditions, suggesting that the aluminum coagulant had virucidal activity (Matsui et al., 2003; Matsushita et al., 2004). However, because we did not confirm whether the floc dissolved completely, it remained unclear whether the change in virus concentration after floc dissolution was the result of the virucidal activity of the aluminum coagulant. To confirm the virucidal activity of the aluminum coagulant, we compared the virus concentration measured by the polymerase chain reaction (PCR) and PFU methods after floc dissolution (Matsushita et al., 2006). The virus concentration determined by the PFU method, which determines the infective virus concentration, was >3 log lower than that determined by the PCR-based method, which determines total virus concentration, regardless of infectivity. This finding suggests that >99.9% of viruses are inactivated by the coagulation process (Matsushita et al., 2006). A similar phenomenon was observed in the

* Corresponding author. Tel./fax: +81 11 706 7279.
E-mail address: taku-m@eng.hokudai.ac.jp (T. Matsushita).

0045-6535/$ - see front matter © 2011 Elsevier Ltd. All rights reserved.
doi:10.1016/j.chemosphere.2011.06.083

supernatant remaining after the coagulation process (Shirasaki et al., 2009a). However, we did not take into account the effect of aggregation of virus particles on the PFU-based concentration: an aggregate consisting of several virus particles are reported to be able to act as one infectious agent (Floyd and Sharp, 1979; Langlet et al., 2007). The production of aggregates, in addition to virus inactivation, is reported to contribute to the difference between the concentrations of viruses determined by the PFU- and PCR-based methods (Langlet et al., 2007; Teunis et al., 2008). In drinking water treatment plants, the water is treated after the coagulation process by further processes, including sedimentation, sand filtration, membrane filtration, chlorination, and UV irradiation. Enmeshment of viruses in aggregates might enhance or reduce the effectiveness of subsequent treatment processes. It is possible that the aggregated virus particles are removed more readily than the monodispersed particles by membrane filtration. However, these aggregates might form a physical barrier to disinfection by chlorination and UV treatment and thus reduce the efficiency of the disinfection process. The aim of our study was to clarify whether or not the difference between the PFU- and PCR-based virus concentrations was the result of virus inactivation or aggregation.

2. Materials and methods

2.1. Bacteriophages used

Three bacteriophages, Qβ (NBRC 20012), MS2 (NBRC 102619) and T4 (NBRC 20004), were obtained from the NITE Biological Resource Center (NBRC, Chiba, Japan). Qβ and MS2 were used as model viruses, whereas T4 was used to investigate the effect of host cell debris on particle size. The diameters of Qβ and MS2 are approximately 23 nm, whereas T4 has a head shell of approximately 65 × 95 nm and a long tail of approximately 25 × 110 nm with six tail fibers.

Escherichia coli F^+ (NBRC 13965) obtained from NBRC was propagated for 3 h at 37 °C according to the supplier's instructions to prepare an *E. coli* F^+ suspension. The bacteriophages were then propagated for 22–24 h at 37 °C in the *E. coli* F^+ suspension. The respective bacteriophage cultures were centrifuged (2000*g*, 10 min) and then filtered through a membrane filter with a pore size of 0.45 μm (cellulose acetate; DISMIC-25cs; Toyo Roshi Kaisya, Tokyo, Japan). The filtrate was purified by using a centrifugal filter device (molecular weight cutoff: 100 000; regenerated cellulose, Amicon Ultra-15; Millipore, Billerica, MA, USA) to prepare the virus stock solution.

2.2. Coagulation and filtration procedure for solutions with low virus concentrations

Batch coagulation experiments were conducted at 20 °C in glass beakers with 200 mL of Qβ- or MS2-spiked (approx. 10^8 PFU mL^{-1}) river water (Toyohira River, Sapporo, Japan; turbidity, 1.0 NTU; dissolved organic carbon concentration, 1.0 mg L^{-1}; OD260, 0.031 cm^{-1}). The river water was mixed with an impeller stirrer, and supplemented with polyaluminum chloride (PACl) (PACl 250A; 10.5% Al_2O_3, relative density 1.2 at 20 °C; Taki Chemical, Hyogo, Japan) or alum (8.1% Al_2O_3, relative density 1.3 at 20 °C; Taki Chemical) at 1.08 mg Al L^{-1}. The water was immediately adjusted to, and maintained at, pH 6.8 with hydrochloric acid or sodium hydroxide. The water was stirred rapidly for 2 min ($G = 200\ s^{-1}$, 61 rpm) and then slowly for 28 min ($G = 20\ s^{-1}$, 13 rpm). The water was then left for 20 min to allow the floc particles to settle. Samples were taken from the beaker before addition of the coagulant and after floc particle settling. The virus concentration was measured after passage of the samples through a membrane filter with a pore size of 50 nm (polycarbonate; VMTP, Millipore). We had measured the virus concentration before and after the filtration of coagulant-free Qβ- and MS2-spiked river water, and found that no reduction in the virus concentration was observed by the filtration, confirming that monodispersed viruses had completely passed through the membrane (data not shown).

2.3. Coagulation and filtration procedure for solutions with high virus concentrations

We measured the particle size of the filtrate to confirm whether or not virus aggregates were present after coagulation. PACl coagulation treatment was conducted with 8 mL of Qβ-spiked (approx 10^{11} PFU mL^{-1}) river water in centrifugal tubes at 20 °C. The river water was supplemented with PACl at predetermined concentrations (0, 54, 81, and 108 mg Al L^{-1}). The pH of the water was immediately adjusted to pH 6.8 by adding hydrochloric acid or sodium hydroxide, the amounts of which were determined in preliminary experiments. The water was then vortexed intensely for 1 min and left for 60 min to allow the floc particles to settle. The water was then centrifuged at 2000*g* for 10 min, and 5 mL of the supernatant was filtered through the 50-nm membrane filter. The particle size was measured with a photon correlation spectrometer (Zetasizer Nano ZS; 532 nm green laser, Malvern Instruments Malvern, Worcestershire, UK) at 25 °C. The same procedure was used for the T4-spiked river water.

2.4. Quantification of bacteriophage concentration

We measured the concentration of infectious bacteriophages by using the agar overlay method (Adams, 1959) with the bacterial host *E. coli* F^+. We determined PFU-based virus concentrations by averaging plaque counts from triplicate plates prepared from one sample.

We quantified the concentration of bacteriophages in samples from extracted viral RNA by the real-time reverse transcription-polymerase chain reaction (RT-PCR) method. This method detects all bacteriophage particles regardless of their infectivity and the existence of aggregates (Langlet et al., 2007). Viral RNA was extracted from 200 μL of sample by using a QIAamp MinElute Virus Spin Kit (Qiagen K. K., Tokyo, Japan). The extracted RNA in a final volume of 20 μL solution was reverse transcribed with a High Capacity cDNA Reverse Transcription Kit with RNase Inhibitor (Applied Biosystems Japan, Tokyo, Japan) at 25 °C for 10 min, 37 °C for 120 min, and 85 °C for 5 s, followed by cooling to 4 °C in a thermal cycler (Thermal Cycler Dice Model TP600, Takara Bio Inc., Shiga, Japan). The cDNA solution was then amplified by using the TaqMan Universal PCR Master Mix with UNG (Applied Biosystems Japan), 400 nM of each primer (HQ-SEQ grade, Takara Bio Inc.), and 250 nM of TaqMan probe (Applied Biosystems Japan). The oligonucleotide sequences of these primers and the probes are listed in Table 1. Amplification was conducted at 50 °C for 2 min, 95 °C for 10 min, and then 40 cycles of 95 °C for 15 s and 60 °C for 1 min in an Applied Biosystems 7300 Real-Time PCR System (Applied Biosystems Japan). The PCR-based viral concentration was expressed as PFU equivalents mL^{-1} as follows. In freshly-prepared stock solutions of the bacteriophages, we assumed that any virus particle possesses infectivity. Accordingly, the PFU equivalent concentration of a sample was determined by converting the number of cycles (C_t value) in the real time RT-PCR amplification of the sample to the PFU concentration according to the relationship between the C_t values and the PFU values for known-concentration freshly-prepared bacteriophage stock solutions.

Table 1
Oligonucleotide sequences of the primers and probes used in real-time RT-PCR quantification of the concentrations of Qβ and MS2 bacteriophages.

Viruses		Oligonucleotide sequence	Position	References
Qβ	Forward primer	5′-TCA AGC CGT GAT AGT CGT TCC TC-3′	49–71	Katayama et al. (2002)
	Reverse primer	5′-AAT CGT TGG CAA TGG AAA GTG C-3′	187–208	
	TaqMan probe	5′-CGA GCC GCG AAC ACA AGA ATT GA-3′	147–169	
MS2	Forward primer	5′-GTC GCG GTA ATT GGC GC-3′	632–648	O'Connell et al. (2006)
	Reverse primer	5′-GGC CAC GTG TTT TGA TCG A-3′	690–708	
	TaqMan probe	5′-AGG CGC TCC GCT ACC TTG CCC T-3′	650–671	

2.5. Electron microscopy

Scanning transmission electron microscopy (SEM, JSM-7400F, JEOL, Tokyo, Japan) was used to analyze the pore size of the membrane used. The pore size of the membrane was expressed as the mean and standard deviation of 16 randomly chosen pores on the electron micrograph.

3. Results and discussion

3.1. Difference in PCR- and PFU-based virus concentrations in filtrate after coagulation

Figure 1 compares the PCR- and PFU-based virus concentrations in the filtrate after passage of the coagulated solutions through the 50-nm membrane filter. Coagulation treatment of Qβ-spiked river water with alum resulted in a 2-log reduction in the viral titer by the PCR-based method from 10^8 to 10^6 PFU equivalents mL^{-1}. By comparison, the same treatment resulted in a 4-log reduction in the viral titer by the PFU-based method to 10^4 PFU mL^{-1}. Thus, the viral concentration in the river water was approximately 100 times (2 logs) as determined by the PCR-based method than by the PFU-based method. When PACl was used as the coagulant, the PFU-based viral concentration of the Qβ-spiked river water was much lower (approx 10^1 PFU mL^{-1}) than when alum was used. However, both coagulants gave the same viral titer with the PCR-based method (approx 10^6 PFU equivalents mL^{-1}). Therefore, coagulation with PACl gave a larger difference (5 logs) in viral titer between the PCR- and PFU-based methods than did alum.

In contrast to our results for Qβ-spiked river water, coagulation treatment of MS2-spiked river water gave a larger reduction in the viral titer by the PCR-based method, to approximately 10^3 and 10^4 PFU mL^{-1} for alum (5 logs) and PACl (4 logs), respectively. However, for the PFU-based method the viral titer for MS2 was approximately 10^2 PFU mL^{-1} for both coagulants; this was almost the same as that obtained for Qβ when PACl was used as the coagulant. These findings agree with those of a previous report (Shirasaki et al., 2009a), in which the PCR-based concentration after in-line coagulation–microfiltration (nominal pore size, 100 nm) was larger for Qβ than for MS2. In summary, we showed that the difference between the PCR- and PFU-based virus concentrations for solutions containing MS2 was smaller than that for solutions containing Qβ, and that for both bacteriophages and coagulants the PCR-based concentration was higher than the PFU-based concentration.

Regardless of the type of virus and coagulant tested, the PFU-based concentration was smaller than the PCR-based concentration. This means that 1 virion detected by the PCR method did not always make one plaque on the host-cell plate in the PFU method. One possible mechanism (Mechanism A) is that some virions became aggregated and behaved as one infectious agent. If this were the case, an aggregate consisting of multiple virions would generate one plaque. In support of this notion Young and Sharp (1977) reported that stocks of poliovirus routinely produced one plaque on host cell monolayers per 100 particles counted. Also Langlet et al. (2007) reported that MS2 exhibited substantial aggregation when the pH was less than or equal to the isoelectric point of 3.9, resulting in the PFU-based concentrations being lower than the PCR-based concentrations; this phenomenon was not observed at pH 6.7. The other possible mechanism (Mechanism B) is that coagulation treatment caused the formation of non-infectious virions. In other words, a part of the virus became inactivated after exposure to hydrolyzing aluminum species during the coagulation process. We previously reported that the virus concentration was lower when determined by the PFU-based method than by the PCR-based method after coagulation with an aluminum coagulant, and we suggested that the virus was inactivated by hydrolyzing aluminum species during the coagulation process (Matsushita et al., 2006; Shirasaki et al., 2007, 2009b).

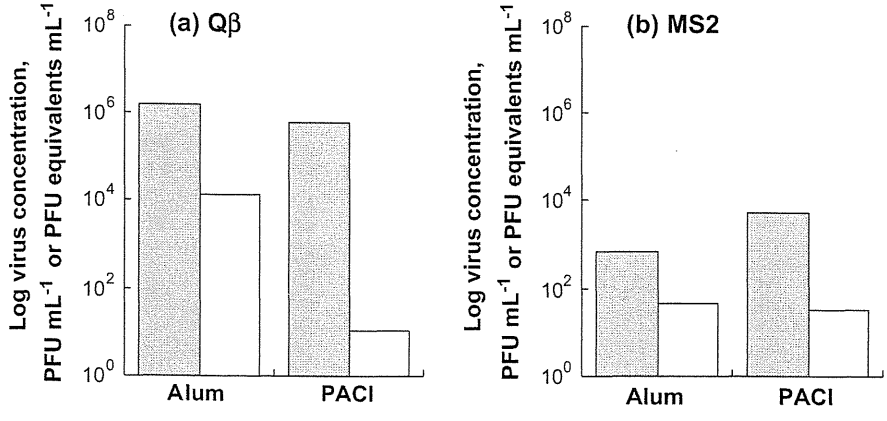

Fig. 1. Comparison of the concentrations of total and infectious viral particles in filtrate (ϕ = 50 nm). Gray and white columns represent PCR-based (i.e., total) and PFU-based (i.e., infectious) virus concentrations. Before coagulation, the initial PCR- and PFU-based concentrations for both the Qβ and MS2 bacteriophages were 10^8 PFU mL^{-1} and 10^8 PFU equivalents mL^{-1}, respectively.

3.2. Aggregate size as an explanation of the difference in PCR-based and PFU-based virus concentrations

If the PFU-based virus concentration is 2 logs lower than the PCR-based virus concentration and the difference between these concentrations can be explained simply by the formation of aggregates that behave as one infectious agent (i.e., Mechanism A), then each aggregate must consist of an average of 10^2 virions. We investigated this hypothesis by calculating the average diameter of the hypothetical aggregate as follows: the ratio of the PCR-based concentration (C_t) to the PFU-based concentration (C_i) after coagulation gave the average number of virions forming one hypothetical aggregate (n).

$$n = \frac{C_t}{C_i} \tag{1}$$

The average number of virions forming one hypothetical aggregate (n) is also expressed as a function of the diameter of the aggregate (R) and that of the virion (r).

$$n = \left(\frac{R}{r}\right)^{D_f} \tag{2}$$

where D_f is the fractal dimension of the aggregate. The following equation is obtained from Eqs. (1) and (2).

$$\frac{C_t}{C_i} = \left(\frac{R}{r}\right)^{D_f} \tag{3}$$

Accordingly,

$$R = \sqrt[D_f]{\frac{C_t}{C_i}}\, r \tag{4}$$

When the fractal dimension of the hypothetical aggregate is 3.0, the aggregate is ideally the most compact and the aggregate diameter is accordingly the smallest. Figure 2 shows the aggregate diameter calculated from the C_i and C_t values in each experiment. For this calculation, we used virion diameters of 23.5 and 22.5 nm for Qβ and MS2, respectively (Shirasaki et al., 2009a), and Df was assumed to be 3.0 (most compact case). We calculated the diameter of aggregates in the PACl-treated solution containing Qβ as 916 nm.

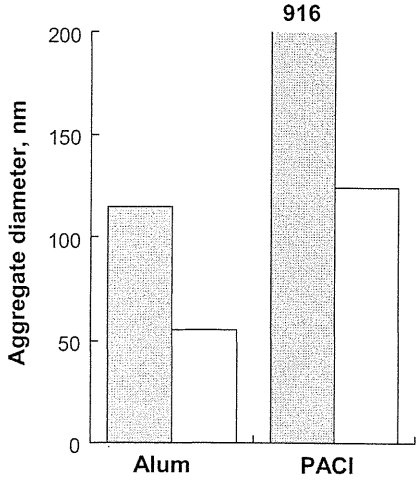

Fig. 2. Aggregate size as an explanation of the difference between PCR- and PFU-based virus concentrations. The fractal dimension of the aggregates is assumed to be 3.0. Gray and white columns represent Qβ and MS2 bacteriophages, respectively.

Because the virus concentration was measured after the samples had been passed through a membrane, the aggregate diameter must have been smaller than the membrane's pore. According to the membrane manufacturer, an electron gun is used to create uniform pores in the membranes, which for the membranes used here were nominally 50 nm. Here, we measured the actual pore of the membrane by using an SEM. Photo 1 is an SEM image of the membrane used for these studies. SEM images of several parts of the membrane revealed that the pores were uniform in size and that abnormally large pores did not exist. We determined the diameter of the pores to be 48.5 ± 3.2 nm, which was consistent with the nominal pore size of the membrane as reported by the manufacturer. Therefore, the 916-nm diameter of aggregates formed by coagulation with PACl was 18 times the 48.5 nm mean pore size of the membrane filter. It is unlikely that aggregates with this diameter could have passed through the membrane's pores, even if they were to change shape because of plasticity. We calculated the diameter of aggregates in the PACl-treated solution containing MS2 and in the alum-treated solution containing Qβ as larger than 100 nm (assuming $D_f = 3.0$); this is more than twice the diameter of the 50-nm pores of the membrane filter. Aggregates of this diameter are also unlikely to pass through a 50-nm membrane filter. This means that the difference in PCR-based and PFU-based virus concentrations of the filtrate was not the result of aggregate formation, or Mechanism A, but was most likely the result of the formation of non-infectious virions by the coagulation process, or Mechanism B. By comparison, the diameter of the aggregates in the alum-treated solution containing MS2 was 55 nm (assuming $D_f = 3.0$), which was almost the same diameter as the pore of the membrane. However, 55 nm was regarded as the minimum possible aggregate size assuming a fractal dimension of 3.0. The fractal dimension of the floc aggregate during the coagulation process changes depending on the operational conditions and is normally smaller than 3.0, with values reported to be 1.5–2.2 (Tambo and Watanabe, 1979; Kim et al., 2001). On the basis of these values, the diameters of the aggregates were 76–135 nm—larger than the pore size of the membrane. Thus, we concluded that, for all four conditions shown in Fig. 1, Mechanism A was implausible, and we propose that Mechanism B explained why the PFU-based virus concentration was lower than the PCR-based virus concentration.

3.3. Measurement of particle size in filtrate after treatment with aluminum coagulant

We provided evidence that any hypothetical aggregate that caused the difference between PCR-based and PFU-based virus concentrations in the filtrate would be larger than the membrane pore. This finding thus suggests that this difference is the result of the formation of non-infectious virions by the coagulation process, or Mechanism B. However, it is also possible that re-aggrega-

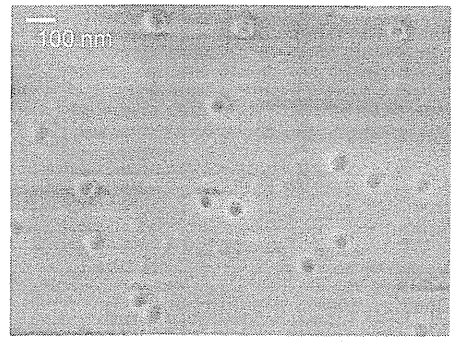

Photo 1. SEM image of the 50-nm membrane filter.

tion of the virus particles occurred after filtration. To investigate this possibility, we directly measured the size of the particles in the filtrate after coagulation treatment with PACl of Qβ- and T4-spiked river water. In these filtrates, the virus concentration of 10^7 PFU equivalents mL^{-1} was below the threshold for detection by photon correlation spectroscopy, so we could not measure particle size. Therefore, we prepared similar solutions with a high virus concentration (approx 10^{11} PFU equivalents mL^{-1}) and subjected them to coagulation treatment with PACl at a concentration higher than the dose routinely used in the treatment of drinking water. We then filtered these solutions and measured the size of the particles in the filtrate.

Particles in the filtrate can be derived from (i) the colloidal materials present in the river water, (ii) the host cell broth, (iii) the host cell debris, and (iv) the virus. We first measured the particle size of the filtrates of the T4-spiked river water. The T4-stock solution contained the T4 bacteriophage, the colloidal materials from host cell broth, and the host cell debris derived from bacteriolytic action. We found that T4 was completely excluded from the filtrate because its diameter was larger than that of the pores of the membrane (data not shown). The filtrate of the T4-spiked river water therefore contained only particles derived from the colloidal material already present in the river water, the host cell broth, and host cell debris. The particles were found to have a mean diameter of approximately 1 nm (0 mg Al L^{-1} white column, Fig. 3) by photon correlation spectrometry. We therefore measured the particle size of filtrates of coagulant-free Qβ-spiked river water and detected particles with a mean diameter of 16.4 ± 0.6 nm (0 mg Al L^{-1} gray column, Fig. 3). Because the particle size of filtrates of coagulant-free Qβ-spiked river water was different from and much larger than that detected in the T4-spiked river water, the particles detected here were unlikely to be the colloidal material present in the river water, the host cell broth, or the host cell debris, and were accordingly most likely Qβ; however, the extent of host cell lysis by Qβ and T4 might have been different and could possibly have accounted for the particles detected in the Qβ-spiked river water. The diameter of 16.4 ± 0.6 nm for Qβ was slightly smaller than the previously reported value of 23.5 ± 0.8 nm based on TEM observation (Shirasaki et al., 2009a). Because the particle size of coagulant-free Qβ-spiked river water before the filtration was almost the same to that after the filtration (data not shown), the filtration process had not damaged the viruses as they were forced through the membrane. Accordingly, the difference in the diameters between the present and the previous studies was possibly because of the difference in the measurement method employed.

We then measured the particle size of filtrates of PACl-treated T4-spiked river water and identified particles with a mean diameter of approximately 1 nm (54 and 108 mg Al L^{-1} white columns, Fig. 3) by photon correlation spectrometry. The size of these particles suggested that floc particles containing T4 must have been removed by filtration and that they were derived from the colloidal material present in the river water, the host cell broth, or host cell debris. We also measured the particle size of filtrates of PACl-treated Qβ-spiked river water and identified particles with a mean diameter of approximately 16 nm (54 and 108 mg Al L^{-1} gray columns, Fig. 3). These particles were substantially larger than those present in PACl-treated T4-spiked river water (1 nm) and were unlikely to have been derived from the colloidal material present in the river water, the host cell broth, or the host cell debris. The diameter of 16 nm was similar to the size of particles detected in the filtrate of the coagulant-free Qβ-spiked river water, suggesting that the particles were Qβ phage particles. Particles larger than 16 nm were not detected in the filtrate. Taken together, these findings suggest that Qβ phage particles in the filtrate remained monodispersed at the tested PACl doses and did not form aggregates.

We compared the PCR- and PFU-based Qβ concentrations in the filtrates of the PACl-treated Qβ-spiked river water (Fig. 4). Although these filtrates contained monodispersed Qβ, the PFU-based concentrations were always lower than those determined by the PCR-based method at all tested PACl doses. These observations clearly showed that the difference between the PCR- and PFU-based Qβ concentrations in the filtrates after coagulation with PACl was attributable to the presence of non-infectious Qβ particles in the filtrate, because aggregates were not detected. The most likely explanation is that the virus became inactivated after exposure to hydrolyzing aluminum species during the coagulation process. The mechanism of virus inactivation by coagulation remains unclear, but it is likely to differ from that underlying virus inactivation by chlorination, ozonation, and UV irradiation. These processes inactivate viruses by modifying the viral genomes or surface proteins. In contrast, it is possible that intermediate polymers formed during hydrolysis of the aluminum coagulants during the coagulation process with aluminum coagulants adsorb to the viruses and physically interfere with their infectivity of host cells. Further study is needed to clarify the mechanisms underlying the inactivation of viruses by aluminum coagulants.

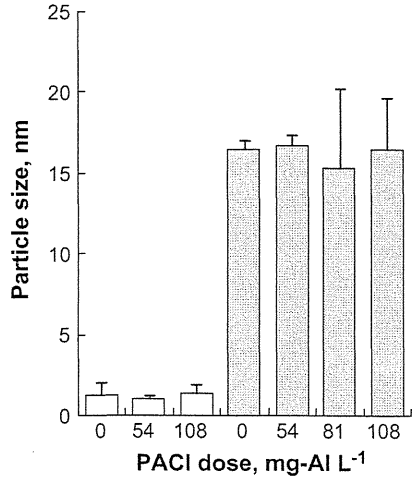

Fig. 3. Mean diameters of particles in filtrate (ϕ = 50 nm) after coagulation with PACl. White and gray columns represent T4- and Qβ-spiked river water, respectively. Error bars represent the standard deviation of 6 measurements.

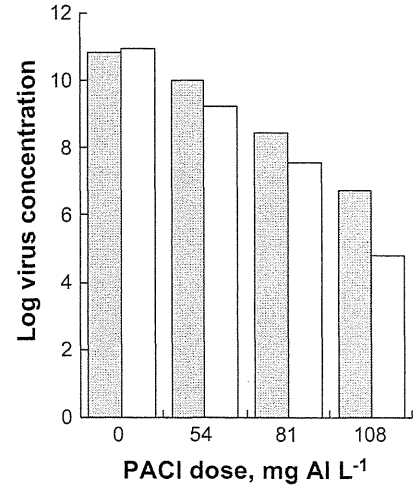

Fig. 4. Comparison of PCR- and PFU-based Qβ concentrations in the filtrate (ϕ = 50 nm) after coagulation with PACl. Gray and white columns represent the PCR- and PFU-based Qβ concentrations, respectively.

4. Conclusions

We used the bacteriophages Qβ and MS2 to determine whether viruses are inactivated by aluminum coagulants during the coagulation process. After filtering the supernatant of the coagulated solution through a membrane with a pore size of 50 nm, the infectious virus concentration was always lower than the total virus concentration. Our particle size measurements revealed that the virus particles in the membrane filtrate were not aggregated but monodispersed, showing that non-infectious Qβ particles were present in the membrane filtrate after the coagulation process with aluminum coagulants. The viruses lost their infectivity after being mixed with hydrolyzing aluminum species during the coagulation process.

Acknowledgments

This research was supported in part by a Grant-in-Aid for the Encouragement of Young Scientists (2010) from the Ministry of Education, Culture, Sports, Science, and Technology of Japan; a Grant-in-Aid (2010) from the Ministry of Health, Labor, and Welfare of Japan; and a Kurita Water and Environment Foundation Research Grant (2009).

References

Adams, M.H., 1959. Bacteriophages. Interscience, New York. pp. 450–454.
Camel, V., Bermond, A., 1998. The use of ozone and associated oxidation processes in drinking water treatment. Water Res. 32, 3208–3222.
Dennis, W.H., Olivieri, V.P., Kruse, C.W., 1979. Mechanism of disinfection: incorporation of Cl-36 into f2 virus. Water Res. 13, 3633–3669.
Floyd, R., Sharp, D.G., 1979. Viral aggregation: buffer effects in the aggregation of Poliovirus and Reovirus at low and high pH. Appl. Environ. Microbiol. 38, 395–401.
Hijnen, W.A.M., Beerendonk, E.F., Medema, G.J., 2006. Inactivation credit of UV radiation for viruses, bacteria and protozoan (oo)cysts in water: a review. Water Res. 40, 3–32.
Katayama, H., Shimazaki, A., Ohgaki, S., 2002. Development of virus concentration method using negatively charged membrane by alkaline elution after acid rinse. J. Jpn. Soc. Water Environ. 25, 469–475 (in Japanese).
Kim, S.H., Moon, B.H., Lee, H.I., 2001. Effects of pH and dosage on pollutant removal and floc structure during coagulation. Microchem. J. 68, 197–203.
Langlet, J., Gaboriaud, F., Gantzer, C., 2007. Effects of pH on plaque forming unit counts and aggregation of MS2 bacteriophage. J. Appl. Microbiol. 103, 1632–1638.
Matsui, Y., Matsushita, T., Sakuma, S., Gojo, T., Mamiya, T., Suzuoki, H., Inoue, T., 2003. Virus inactivation in aluminum and polyaluminum coagulation. Environ. Sci. Technol. 37, 5175–5180.
Matsushita, T., Matsui, Y., Inoue, T., 2004. Irreversible and reversible adhesions between virus particles and hydrolyzing-precipitating aluminum: a function of coagulation. Water Sci. Technol. 50 (12), 201–206.
Matsushita, T., Matsui, Y., Shirasaki, N., 2006. Analyzing mass balance of viruses in a coagulation-ceramic microfiltration hybrid system by a combination of the polymerase chain reaction (PCR) method and the plaque forming units (PFU) method. Water Sci. Technol. 53 (7), 199–207.
O'Connell, K.P., Bucher, J.R., Anderson, P.E., Cao, C.J., Khan, A.S., Gostomski, M.V., Valdes, J.J., 2006. Real-time fluorogenic reverse transcription-PCR assays for detection of bacteriophage MS2. Appl. Environ. Microbiol. 72, 478–483.
Shirasaki, N., Matsushita, T., Matsui, Y., Ohno, K., Kobuke, M., 2007. Virus removal in a hybrid coagulation–microfiltration system—Investigating mechanisms of virus removal by a combination of PCR and PFU methods. Water Sci. Technol.:. Water Supply 7 (5–6), 1–8.
Shirasaki, N., Matsushita, T., Matsui, Y., Kobuke, M., Ohno, K., 2009a. Comparison of removal performance of two surrogates for pathogenic waterborne viruses, bacteriophage Qβ and MS2, in a coagulation–ceramic microfiltration system. J. Membrane Sci. 326, 564–571.
Shirasaki, N., Matsushita, T., Matsui, Y., Urasaki, T., Ohno, K., 2009b. Comparison of behaviors of two surrogates for pathogenic waterborne viruses, bacteriophages Qβ and MS2, during the aluminum coagulation process. Water Res. 43, 605–612.
Tambo, N., Watanabe, Y., 1979. Physical characteristics of flocs—I. The floc density function and aluminum floc. Water Res. 13, 409–419.
Teunis, P.F.M., Moe, C.L., Liu, P., Miller, S.E., Lindesmith, L., Baric, R.S., Pendu, J.L., Calderon, R.L., 2008. Norwalk virus: how infectious is it? J. Med. Virol. 80, 1468–1476.
USEPA, Contaminant Candidate List 3 – CCL <http://water.epa.gov/scitech/drinkingwater/dws/ccl/ccl3.cfm.>.
Young, D.C., Sharp, D.G., 1977. Poliovirus aggregates and their survival in water. Appl. Environ. Microbiol. 33, 168–177.

ANALYTICAL SCIENCES NOVEMBER 2011, VOL. 27

Analysis of Bromate in Drinking Water Using Liquid Chromatography-Tandem Mass Spectrometry without Sample Pretreatment

Koji KOSAKA,*† Mari ASAMI,* Kanako TAKEI,* and Michihiro AKIBA**

**Water Management Section, Department of Environmental Health, National Institute of Public Health, 2-3-6 Minami, Wako, Saitama 351-0197, Japan*
***National Institute of Public Health, 2-3-6 Minami, Wako, Saitama 351-0197, Japan*

An analytical method for determining bromate in drinking water was developed using liquid chromatography-tandem mass spectrometry (LC-MS/MS). The ^{18}O-enriched bromate was used as an internal standard. The limit of quantification (LOQ) of bromate was 0.2 μg/L. The peak of bromate was separated from those of coexisting ions (*i.e.*, chloride, nitrate and sulfate). The relative and absolute recoveries of bromate in two drinking water samples and in a synthesized ion solution (100 mg/L chloride, 10 mg N/L nitrate, and 100 mg/L sulfate) were 99 - 105 and 94 - 105%, respectively. Bromate concentrations in 11 drinking water samples determined by LC-MS/MS were <0.2 - 2.3 μg/L. The results of the present study indicated that the proposed method was suitable for determining bromate concentrations in drinking water without sample pretreatment.

(Received May 8, 2011; Accepted September 20, 2011; Published November 10, 2011)

Introduction

Bromate may be carcinogenic in humans and is listed as Group 2B by the International Agency for Research on Cancer (IARC).[1] Bromate is known to be a disinfection by-product during ozonation.[2] It has also been reported that bromate is present as an impurity in sodium hypochlorite solution, a disinfectant.[3,4] The maximum contaminant level (MCL) of bromate in drinking water in the United States of America (USA) is 10 μg/L.[5] The guideline value in the World Health Organization (WHO) Guidelines for drinking water quality and the standard value in drinking water in Japan are 10 μg/L.[6,7]

To determine bromate concentration in drinking water at low concentration, ion chromatography-postcolumn reaction (IC-PCR) has been applied.[8-11] This method is selected as an official method for drinking water in Japan.[12] However, maintenance of the postcolumn module was difficult because high concentrations of sulfate solution and other chemicals were used. Recently, in the IC system, mass spectrometry (MS) has been applied to determine bromate. The methods using both MS (*i.e.*, IC-MS)[13-15] and tandem mass spectrometry (*i.e.*, IC-MS/MS)[16-20] were reported, but the number of studies using IC-MS/MS, a more accurate method, seemed to be larger. Also, more recently, liquid chromatography (LC)-MS/MS has been applied for bromate analysys.[21,22] Although IC-MS/MS and LC-MS/MS are highly sensitive and accurate, these methods have a problem for the application in drinking water. That is, when coexisting ions (*e.g.*, chloride, nitrate and sulfate) contained in drinking water co-eluted with bromate, ion suppression or ion enhancement occurred, which resulted in reduction or increase of the sensitivity. Thus, for the determination of bromate in drinking water using IC-MS/MS or LC-MS/MS, it is necessary to chromatographically separate bromate from coexisting ions, particularly chloride for IC, or to mitigate their effects with sample pretreatment. In the case of IC-MS/MS, chromatographic separation was occasionally achieved and bromate were determined without sample pretreatment.[19,20] On the other hand, in the case of LC-MS/MS, no methods for analysis of bromate without pretreatment have yet been reported. As examples of the sample pretreatment methods, pretreatment cartridges have been used to remove coexisting ions from water.[21] In addition, sample dilution was performed to reduce the effects of coexisting ions and to determine oxyhalide including bromate in sodium hypochlorite solution.[22] In this previous study,[22] ^{18}O-enriched perchlorate and bromate were used as internal standards of perchlorate and bromate, respectively. From these reports, we considered that IC-MS/MS might be more suitable than LC-MS/MS to determine ions including bromate in drinking water. However, compared to LC-MS/MS, more components such as a suppressor and an auxiliary pump are needed for IC-MS/MS. Also, in Japan, application of IC-MS/MS is limited in water utilities and institutions for water quality tests. Therefore, we considered that the development of an analytical method for bromate using LC-MS/MS without pretreatment would be very useful.

In the present study, we developed a method for analysis of bromate in drinking water using LC-MS/MS without the need for sample pretreatment. Bromate concentrations in drinking water were determined using the proposed method.

† To whom correspondence should be addressed.
E-mail: kosaka@niph.go.jp

Table 1 Compound-dependent parameter of MS/MS

Compound	Precursor ion (*m/z*)	Product ion (*m/z*)	Declustering potential/ V	Collision energy/ V	Collision cell exit potential/V
Bromate	126.884	110.700	–45	–30	–2
^{18}O-Enriched bromate	132.893	114.800	–45	–30	–2
Chloride	35.000	35.000	–20	–6	–4
Nitrate	62.014	46.100	–30	–30	–4
Sulfate	96.956	79.900	–50	–28	0

Experimental

Reagents and solutions

Ultrapure water purified using a Gradient A10 water purification system (Millipore, Bedford, MA) was used for the experiments (*e.g.*, preparations of the standard and stock solutions and eluents). Standard bromate solution was purchased from Kanto Chemical (Tokyo, Japan), and those of chloride, nitrate, sulfate and chlorite were purchased from Wako Pure Chemicals (Osaka, Japan). Standard haloacetic acid solutions containing nine types of haloacetic acids were purchased from Kanto Chemical. ^{18}O-Enriched potassium bromate solution was purchased from Cambridge Isotope Laboratories (Andover, MA). All other reagents used in the present study were of analytical grade.

Sample preparation and recovery studies

The ^{18}O-enriched bromate was added to the samples as an internal standard and mixed before analysis (final concentration, 2.0 μg/L). Bromate recovery studies were performed using two types of drinking water (*i.e.*, drinking waters A and B) and synthesized ion water. Drinking water samples A and B were tap water collected in Saitama and Chiba prefectures, respectively. Ammonium chloride (Sigma-Aldrich, St. Louis, MO) was added in drinking water (final concentration, 20 mg/L) to transform residual chlorine into chloramines.[20] The synthesized ion water was prepared by dissolving 100 mg/L of chloride, 10 mg N/L of nitrate and 100 mg/L of sulfate in ultrapure water. For all recovery studies, spiked bromate concentration was 1.0 μg/L. Separation of bromate and haloacetic acids or chlorite was also investigated. Moreover, 11 drinking water samples were collected in June and July 2010 to determine bromate levels in drinking water. The two drinking water samples used for recovery studies were not included in the 11 drinking water samples. As was the case in the recovery studies described above, ammonium chloride was added in drinking water to transform residual chlorine into chloramines. All the sample solutions collected were refrigerated at 4°C.

Analytical methods

Bromate concentrations in water samples were determined by LC-MS/MS. The separation was performed using an Agilent 1200SL binary pump (Agilent Technologies, Palo Alto, CA). The separation column used was an Acclaim Trinity P1 column (3.0 mm × 100 mm, 3 μm; Dionex, Sunnyvale, CA); its temperature was 30°C. This column has reversed-phase, anion-exchange and cation-exchange retention properties.[23] Eluent A was a 40/60 (v/v) mixture of 20 mM ammonium acetate (Wako Pure Chemicals) and 0.05% (v/v) acetic acid (Wako Pure Chemicals) aqueous solution (pH 5)/acetonitrile (high-performance liquid chromatography grade; Wako Pure Chemicals). Eluent B was a 90/10 (v/v) mixture of 200 mM ammonium acetate and 0.5% (v/v) acetic acid aqueous solution (pH 5)/acetonitrile. The gradient conditions of eluent B were as follows: 0% held for 9 min, a linear increase to 95% in 0.5 min and held for 10 min, a linear decrease to 0% in 0.5 min and held for 6 min. After each run, the eluents were flowed for 1 min under the initial conditions. The total run time of each sample was 27 min. The flow rate was 0.7 mL/min, and the injection volume was 50 μL. Detection was performed using a 3200 QTRAP tandem mass spectrometer (Applied Biosystems, Foster City, CA) operated in the negative-ion turbo ion spray mode. In the present study, only MS/MS was investigated and the comparison between MS and MS/MS was not performed. This is because MS/MS is known to be more accurate and the investigation of the analytical conditions without sample pretreatment was considered to be a more interesting topic. The analytical conditions of the tandem mass spectrometer were optimized for bromate analysis. Collision gas flow was 6 psig, curtain gas flow was 30 psig, ion source gas 1 flow was 70 psig, ion source gas 2 flow was 60 psig, ionspray voltage was –4500 V and temperature was 700°C. The multiple reaction monitoring (MRM) transitions were *m/z* 127 ($^{79}BrO_3^-$) to *m/z* 111 ($^{79}BrO_2^-$) for bromate and *m/z* 133 ($^{79}Br^{18}O_3^-$) to *m/z* 115 ($^{79}Br^{18}O_2^-$) for ^{18}O-enriched bromate. The details of the compound-dependent parameters of MS/MS are shown in Table 1. In some cases, the peaks of chloride, nitrate and sulfate were monitored. These MRM transitions were *m/z* 35 ($^{35}Cl^-$) to *m/z* 35 ($^{35}Cl^-$), *m/z* 62 (NO_3^-) to *m/z* 46 (NO_2^-) and *m/z* 97 (HSO_4^-) to *m/z* 80 (SO_3^-), respectively.

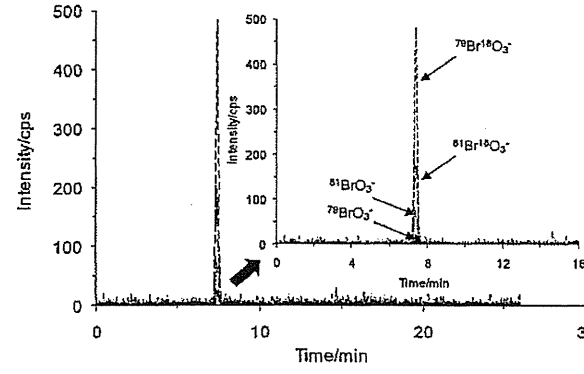

Fig. 1 MRM chromatograms of ^{18}O-enriched bromate at 10 μg/L in ultrapure water.

Results and Discussion

Optimization of analytical conditions of bromate and its limit of quantification

Figure 1 shows the MRM chromatograms of ^{18}O-enriched bromate at 10 μg/L in ultrapure water samples. The ^{18}O-enriched bromate has two isotopes (*i.e.*, $^{79}Br^{18}O_3^-$ and $^{81}Br^{18}O_3^-$). The background of the chromatogram of $^{81}Br^{18}O_3^-$ was higher than that of $^{79}Br^{18}O_3^-$. Thus, the peak area of $^{81}Br^{18}O_3^-$ was lower than that of $^{79}Br^{18}O_3^-$ although the isotope abundance ratios were similar. That is, *m/z* 133 ($^{79}Br^{18}O_3^-$) to *m/z* 115 ($^{79}Br^{18}O_2^-$) was used for the MRM transition of ^{18}O-enriched bromate. Also, 10 μg/L of ^{18}O-enriched bromate solution had bromate peaks ($^{79}BrO_3^-$ and $^{81}BrO_3^-$) although the peak areas were lower

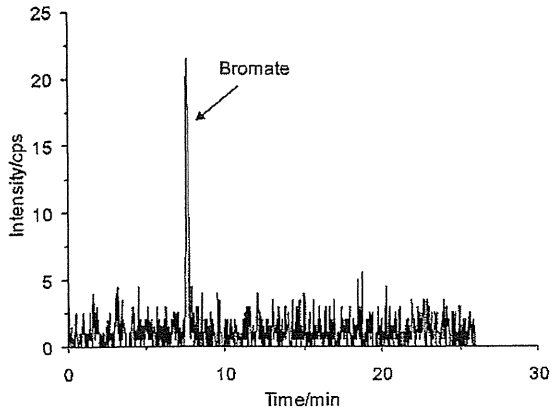

Fig. 2 MRM chromatograms of bromate at 0.2 μg/L in ultrapure water.

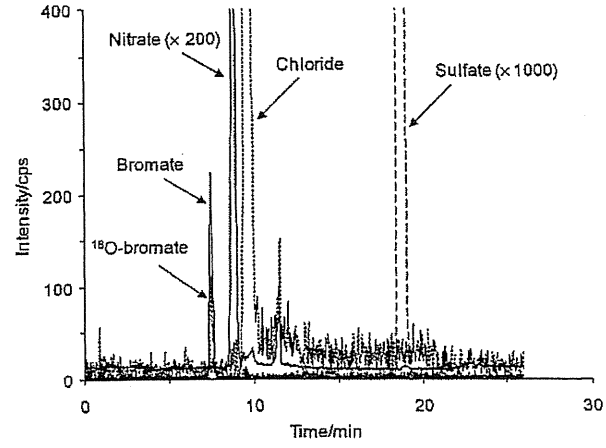

Fig. 3 MRM chromatograms of bromate, chloride, nitrate and sulfate in drinking water.

Table 2 Recovery of bromate in matrix solution ($n = 3$)[a]

Matrix	Native bromate concentration/μg L^{-1}	Relative recovery, %[b,c]	Absolute recovery, %[c]
Drinking water A	<0.2	105 (3.7)	102 (1.0)
Drinking water B	0.4	109 (4.0)	105 (1.0)
Synthesized ion water	—	99 (1.6)	94 (5.5)

a. Spiked bromate concentration was 1.0 μg/L.
b. Recovery corrected by ^{18}O-enriched bromate.
c. Values in parentheses are relative standard deviations (RSDs).

than that of ^{18}O-enriched bromate. The peak area of $^{81}BrO_3^-$ was higher than that of $^{79}BrO_3^-$. In the previous study, the presence of the bromate peak in ^{18}O-enriched bromate solution was not described.[22] Note that the supplier in the previous study was different from that in the present study. When ^{18}O-enriched bromate concentration was reduced to 2.0 μg/L, the peak of $^{79}BrO_3^-$ was not observed. Thus, in the present study, the ^{18}O-enriched bromate concentration added to the sample solution as an internal standard was set to 2.0 μg/L. In the case of bromate, the MRM transition of $^{79}BrO_3^-$ was selected for monitoring.

The bromate calibration points were set at 0.2, 0.5, 1.0, 5.0, and 10 μg/L, and the calibration curve was linear ($R^2 > 0.998$). The method detection limit (MDL) of bromate was determined by repeated analyses ($n = 7$) of 0.2 μg/L of bromate in ultrapure water. Figure 2 shows the MRM chromatograms of bromate at 0.2 μg/L in ultrapure water. The bromate retention time was ~7.5 min. The mean bromate concentration was 0.22 μg/L and its standard deviation (SD) was 0.019 μg/L. The value of 10 × SD was 0.19 μg/L, and therefore the limit of quantification (LOQ) of bromate was set at 0.2 μg/L. It was reported previously that, in the case of IC-MS/MS, the LOQ of bromate was 0.05 μg/L,[21] and the lowest concentration minimum reporting level (LCMRL) was calculated as 0.042 μg/L.[20] It was also reported that the LOQ for bromate using LC-MS/MS was 0.1 μg/L.[18] Thus, the LOQ and LCMRL of bromate using LC-MS/MS in the present study were higher than those in previous studies. On the other hand, the LOQ of the conventional method, IC-PCR, is 0.2 μg/L.[24] The target value for bromate (*e.g.*, MCL in the USA, the guideline value in WHO Guideline for drinking water quality, and a standard value in Japan) is 10 μg/L in many cases.[5-7] Therefore, the LOQ of bromate in the present study was sufficient to determine bromate in drinking water.

Recovery studies of bromate

Next, bromate recovery was investigated ($n = 3$). Table 2 shows the results of bromate in matrix solutions (*i.e.*, two samples of drinking water and synthesized ion water). The mean relative recoveries of bromate were in the range of 99 - 105%. The relative standard deviations (RSDs) were 1.6 - 4.0%. The mean absolute recoveries of bromate were also high (*i.e.*, 94 - 105%), and the RSDs were 1.0 - 5.5%. The addition of ammonium chloride did not affect the recoveries of bromate in drinking water. Thus, we showed that, using the proposed method, sample pretreatment (*e.g.*, using pretreatment cartridges) was not required to determine bromate concentrations.

Separation of bromate with coexisting compounds

Figure 3 shows MRM chromatograms of bromate and coexisting ions (*i.e.*, chloride, nitrate and sulfate) in drinking water. In the case of IC, the chloride retention time is generally shorter than that of nitrate. The bromate peak occasionally overlaps with that of chloride. However, in the present study, the bromate peak was separated from those of chloride, nitrate and sulfate. In addition, the nitrate retention time was shorter than that of chloride. The column used has the multiple retention properties[23] and we considered that the separation of the ions was obtained by the combined effects of these properties. Thus, we presumed that the separation mechanism of the ions by the column used was different from that by IC although the main mechanism was unclear. This chromatographic separation was considered to be one reason for the high recoveries of bromate observed in the present study (Table 2). In the present study, the gradient condition of LC was changed back to the initial state (*i.e.*, 0% of eluent B) after the elution of sulfate (Fig. 3). We considered that the retention times of some compounds in drinking water are longer than that of sulfate. For example, the retention times of some haloacetic acids were longer than that of sulfate in IC-MS/MS system.[18-20] Elution of nine haloacetic acids were investigated under the condition that the final gradient conditions in the present study (*i.e.*, 95% of

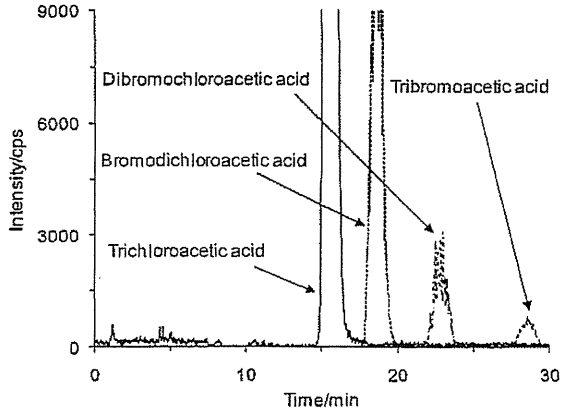

Fig. 4 MRM chromatograms of some haloacetic acids at 5 mg/L in ultrapure water.

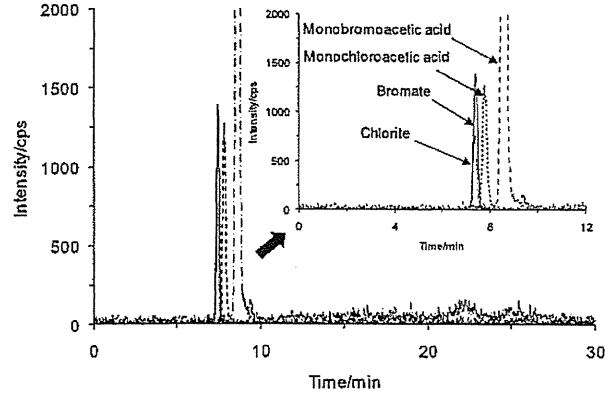

Fig. 5 MRM chromatograms of bromate (10 μg/L), chlorite (100 μg/L), monochloroacetic acid (100 μg/L) and monobromoacetic acid (100 μg/L) in ultrapure water.

eluent B) were continued. As in the case of IC-MS/MS system,[18-20] the retention times of trihaloacetic acids were longer than those of mono- and dihaloacetic acids (data not shown). The retention time of tribromoacetic acid was around 30 min and was the slowest among the four trihaloacetic acids (Fig. 4). In the figure, the MRM transitions of trichloroacetic acid, bromodichloroacetic acid, dibromochloroacetic acid and tribromoacetic acid were *m/z* 161 ($C^{35}Cl_3COO^-$) to *m/z* 117 ($C^{35}Cl_3^-$), *m/z* 161 ($C^{79}Br^{35}Cl_2^-$) to *m/z* 79 ($^{79}Br^-$), *m/z* 209 ($C^{81}Br_2^{35}Cl^-$) to *m/z* 81 ($^{81}Br^-$) and *m/z* 251 ($C^{79}Br_2^{81}Br^-$) to *m/z* 79 ($^{79}Br^-$), respectively. The temperature of the MS/MS system was set at 300°C in Fig. 4. This value was lower than that of the analytical conditions of bromate (*i.e.*, 700°C) (see section of analytical methods). This is because the sensitivities of the trihaloacetic acids in the MS/MS system were low at 700°C, and their peaks were not observed. It was considered that trihaloacetic acids were easy to degrade by thermal decomposition. The result in Fig. 4 indicated that the longer gradient condition of 95% of eluent B seemed to be better from the point of the accumulation of compounds in the column. However, as described above, the recovery of bromate in the gradient conditions used in the present study was high (Table 2). Thus, this gradient condition in the present study was employed. Moreover, it was reported that the peak of bromate was close to that of monobromoacetic acid and was relatively close to those of monochloroacetic acid and chlorite in IC-MS/MS system.[13] In LC-MS/MS system, the peak of bromate was close to that of monochloroacetic acid and was relatively close to that of monobromoacetic acid (Fig. 5). In the figure, the MRM transitions of monochloroacetic acid, monobromoacetic acid and chlorite were *m/z* 93 ($C^{35}ClH_2COO^-$) to *m/z* 35 ($^{35}Cl^-$), *m/z* 139 ($C^{81}BrH_2COO^-$) to *m/z* 81 ($^{81}Br^-$) and *m/z* 67 ($^{35}ClO_2^-$) to *m/z* 51 ($^{35}ClO^-$), respectively. On the other hand, the peak of bromate was overlapped with that of chlorite. In drinking water regulation in Japan, chlorite is selected as the management item and its target value is 600 μg/L.[12] Our results suggested that it was difficult to determine bromate using the proposed method without sample pretreatment in the samples containing chlorite at high concentration, although chlorite concentration in drinking water is generally low.

Application in drinking water samples

Moreover, the bromate concentrations in 11 drinking water samples were determined using LC-MS/MS. Three drinking water samples had conventional purification systems (*i.e.*, coagulation, flocculation and sand filtration). Bromate was detected in two of the three drinking water samples, and its concentrations were <0.2 - 0.4 μg/L. The purification systems of the remaining eight drinking water samples involved conventional purification systems with ozone/biological activated carbon (BAC) treatment. Bromate was detected in all eight drinking water samples at concentrations in the range 0.5 - 2.3 μg/L. These results were in agreement with those of previous studies indicating that bromate is produced during ozonation.[2] The absolute recoveries of ^{18}O-enriched bromate in the 11 drinking water samples were 94 - 101%. The results of the present study indicated that the proposed LC-MS/MS method is applicable for determination of bromate concentrations in drinking water without sample pretreatment.

Conclusions

(1) The LOQ of bromate using LC-MS/MS with ^{18}O-enriched bromate as an internal standard was 0.2 μg/L.
(2) The relative and absolute recoveries of bromate in two drinking water samples and one synthesized ion solution were 99 - 105 and 94 - 105%, respectively.
(3) Bromate concentrations in 11 drinking water samples determined using LC-MS/MS were <0.2 - 2.3 μg/L. The proposed method using LC-MS/MS was applicable to determination of bromate in drinking water without sample pretreatment.

Acknowledgements

The authors greatly thank Dr. Y. Sekiguchi (Dionex) and Mr. T. Suzuki (Dionex) for advice on chromatographic conditions. The present study was financially supported in part by a research grant from the Ministry of Health, Labour and Welfare, Japan.

References

1. IARC Monographs on the Evaluation of Carcinogenic Risks to Humans Volume 73, "Some chemicals that cause tumours of the kidney or urinary bladder in rodents and

some other substances", **1999**.
2. U. von Gunten, *Water Res.*, **2003**, *37*, 1469.
3. H. S. Weinberg, C. A. Delcomyn, and V. Unnam, *Environ. Sci. Technol.*, **2003**, *37*, 3104.
4. M. Asami, K. Kosaka, and S. Kunikane, *J. Water Supply Res. Technol.—Aqua*, **2009**, *58*, 107.
5. US Environmental Protection Agency, Stage 2 Disinfectants and Disinfection Byproducts Rule, **2006**.
6. WHO, Guidelines for Drinking-water Quality, 3rd ed., **2006**.
7. Water Supply Division, Health Bureau, Ministry of Health, Labour, and Welfare (in Japanese), http://www.mhlw.go.jp/topics/bukyoku/kenkou/suido/suishitsu/06.html.
8. Y. Inoue, T. Sakai, H. Kumagai, and Y. Hanaoka, *Anal. Chim. Acta*, **1997**, *346*, 299.
9. H. S. Weinberg and H. Yamada, *Anal. Chem.*, **1998**, *70*, 1.
10. E. Salhi and U. von Gunten, *Water Res.*, **1999**, *33*, 3239.
11. H. P. Wagner, B. V. Pepich, D. P. Hautman, and D. J. Munch, *J. Chromatogr, A*, **2002**, *956*, 93.
12. Water Supply Division, Health Bureau, Ministry of Health, Labour, and Welfare (in Japanese), http://www.mhlw.go.jp/topics/bukyoku/kenkou/suido/kijun/kijunchi.html.
13. R. Roehl, R. Slingsby, N. Avdalovic, and P. E. Jackson, *J. Chromatogr., A*, **2002**, *2002*, 245.
14. S. Cavalli, S. Polesello, and S. Valsecchi, *J. Chromatogr., A*, **2005**, *1085*, 42.
15. L. Barron and B. Paull, *Talanta*, **2006**, *69*, 621.
16. L. Charles and D. Pépin, *J. Chromatogr., A*, **1998**, *804*, 105.
17. L. Charles and D. Pépin, *J. Chromatogr., A*, **1998**, *70*, 353.
18. M. Asami, K. Kosaka, Y. Matsuoka, and M. Kamoshita, *J. Environ. Chem.* (in Japanese), **2007**, *17*, 363.
19. H. Li, T. Suzuki, and Y. Sekiguchi, *Industrial Water* (in Japanese), **2008**, *591*, 56.
20. US Environmental Protection Agency, Method 557: Determination of haloacetic acids, bromate, and dalapon in drinking water by ion chromatography electrospray ionization tandem mass spectrometry (IC-ESI-MS/MS), **2009**.
21. S. A. Snyder, B. J. Vanderford, and D. J. Rexing, *Environ. Sci. Technol.*, **2005**, *39*, 4586.
22. A. N. Pisarenko, B. D. Stanford, O. Quiñones, G. E. Pacey, G. Gordon, and S. A. Snyder, *Anal. Chim. Acta*, **2010**, *659*, 216.
23. Dionex, Acclaim Trinity P1 LC Column, http://www.dionex.com/en-us/webdocs/70761-DS-Acclaim-Trinity-12Feb2010-LPN2239-02.pdf.
24. S. Itoh and S. Echigo, "*Disinfection Byproducts in Water* (in Japanese)", **2008**, Gihodo Shuppan, Tokyo.

土木学会論文集G（環境），Vol.67，No.7，III_13-III_21，2011.

（2） 水道におけるN-ニトロソアミン類とその前駆物質の実態調査

小坂　浩司[1*]・廣瀬　一人[1,2]・浅見　真理[1]・秋葉　道宏[3]

[1]国立保健医療科学院生活環境研究部水管理研究分野（〒351-0197 埼玉県和光市南2-3-6）

[2]厚生労働省健康局水道課（〒100-8916 東京都千代田区霞ヶ関1-2-2）

[3]国立保健医療科学院（〒351-0197 埼玉県和光市南2-3-6）

＊ E-mail: *kosaka@niph.go.jp*

全国19浄水場を対象に，夏季，冬季の原水と浄水中の3種のN-ニトロソアミン類（N-ニトロソジメチルアミン（NDMA），N-ニトロソモルホリン（NMor），N-ニトロソピロリジン（NPyr））の実態調査を行った．原水，浄水中のNDMAは，それぞれ延べ36試料中11試料，36試料中9試料から検出された．NMorはそれぞれ延べ36試料中4試料，36試料中4試料から検出された．NPyrはいずれの試料からも検出されなかった．下水処理場放流水と事業所排水口直下の水路の水の場合，NDMAとNMorは，10試料全てから検出され，NPyrは検出されなかった．原水や排水をクロラミン処理，オゾン処理したところ，NDMAの場合，クロラミン処理後の方が濃度が増加した試料数は多かった．NMorの場合，いずれの処理後でも濃度は増加せず，NPyrは，一部の排水試料において，クロラミン処理後に濃度が増加した．3試料を対象に，オゾン処理時間とNDMAの生成との関係について検討した結果，試料によって時間は異なったが，いずれも溶存オゾンが検出され始めるまでの処理時間に設定すると，NDMAの生成量は最大になることがわかった．

Key Words : N-nitrosamines, N-nitrosodimethylamine (NDMA), N-nitrosamine precursors, chloramination, ozonation, water supply

1. はじめに

N-ニトロソジメチルアミン（NDMA）は，国際がん研究機関（IARC）においてグループ2A（ヒトに対しておそらく発がん性がある）[1]に，統合的リスク情報システム（IRIS）においてクラスB2（人に対して発がんの可能性がある）[2]に分類されている．また，IRISは10^{-5}の生涯発がんリスクに相当する飲料水中濃度として7 ng/L[2]を，世界保健機関（WHO）は飲料水中のガイドライン値として100 ng/L[3]を示している．国内の飲料水に係わる規制では，要検討項目に指定され，目標値として100 ng/L[4]が定められている．

NDMA以外の複数のN-ニトロソアミン類も，IARCでグループ2Aやグループ2B（人に対する発がん性が疑われる）[1]に，IRISでクラスB2[5]に分類されている．また，米国環境保護庁（USEPA）の第3次未規制物質候補リスト（CCL3）[6]にNDMAを含む5種のN-ニトロソアミン類が，第2次未規制物質監視規則（UCMR2）[7]にNDMAを含む6種のN-ニトロソアミン類が指定されている．

海外では，NDMAに関する研究は，カナダ[8]やカリフォルニア州[9]の飲料水中から検出されて以降，実態調査や新規の消毒副生成物としてクロラミン処理による生成機構等が，複数の研究者によって進められてきた[8),10)-16)]．また，NDMAは，オゾン処理による副生成物でもあることも報告された[17),18)]．また，当初は，N-ニトロソジメチルアミンのうち，NDMAに対する研究が主であったが，それ以外のN-ニトロソジメチルアミン類についての調査研究も行われている[19)-21)]．

国内では，NDMAに関する研究は，数年前から幾つか報告が行われてきた．例えば，全国の浄水場や浄水プロセスにおけるNDMAの実態調査[22)]，淀川流域や利根川流域を対象とした下水処理場放流水や河川水中の実態調査[23)-25)]，東京の地下水中のNDMAの実態調査[26)]等が挙げられる．また，NDMAの前駆物質に係わる研究では，淀川流域では，下水処理場放流水中にオゾン処理によるNDMA前駆物質が含まれていることも明らかとなってい

る[22,23,27]．一方，NDMA以外のN-ニトロソアミン類に関する調査研究は，淀川流域の浄水場，上流の下水処理場放流水，河川水等について行われているが[5,28]，報告は少ない．このため，N-ニトロソアミン類やクロラミン処理，オゾン処理による前駆物質について，全国的な存在状況の把握することは，重要であると考えられる．

また，現状，国内水道では，クロラミン処理を採用している浄水場はごく一部に限られ，浄水中でNDMA濃度が相対的に高い濃度で検出された浄水場は，特に冬季の淀川流域のオゾン処理を導入している浄水場であった[22]．これらのことから，国内水道では，オゾン処理によるNDMAの生成が課題となっていると考えられるが，その生成能を評価する際，どのような条件で実施したら適切であるか明らかになっていない．試験室ごとで，反応槽や対象水が異なることから，オゾン処理条件に対する何らかの共通の目安を示すことができれば，非常に有用であると考えられる．

本研究は，全国の浄水場を対象に，N-ニトロソアミン類について調査を行った．N-ニトロソアミン類として，NDMA およびこれまでの国内外の調査を参考にして，N-ニトロソモルホリン（NMor），N-ニトロソピロリジン（NPyr）を対象とした．また，浄水場の上流域にある下水処理場等の排水についても同様に調査した．クロラミン処理やオゾン処理による影響についても検討し，前駆物質の調査を行った．さらに，オゾン処理によるN-ニトロソアミン類の生成を評価する際の処理条件についても検討した．

2. 実験方法

(1) 試薬および保存溶液

NDMA，NMor，NPyrの標準液は，Supelcoから購入した．NDMA-d_6はC/D/N Isotopesから購入し，NMor-d_8およびNPyr-d_8はCambridge Isotope Laboratoriesから購入した．クロラミン溶液は，次亜塩素酸ナトリウム溶液とpH 8.5に調製した塩化アンモニウム溶液を1：1.2 mol/molで混合させ，冷蔵庫で1～2時間静置させた後，実験に使用した[20]．クロラミン溶液は，実験日ごとに作成した．各溶液の調製には，Gradient A10（Millipore）で精製した超純水を使用した．ただし，超高速液体クロマトグラフタンデム質量分析計（UPLC-MS/MS）の溶離液の場合のみ蒸留水（LC-MS用，関東化学）を使用した．

(2) 試料の採取

2010年7～9月（夏季）と2011年1，2月（冬季）に，全国の19浄水場（A～S浄水場）の原水と浄水を採取し，N-ニトロソアミン類濃度の測定を行った．ただし，F，H，N浄水場は冬季の調査は行わず，O浄水場は夏季については2回調査を行った．5浄水場（F，G，H，N，O浄水場）については，プロセス水の調査も実施した（O浄水場の夏季調査の場合，プロセス水の調査は2回のうち1回のみ）．これら浄水場は，高度浄水プロセス（オゾン/活性炭処理）を採用している．原水の場合，F浄水場を除き，クロラミン処理による影響についての調査も行った．

2010年11，12月，淀川流域の5下水処理場放流水（a～e下水処理場，b下水処理場については2放流口があったためb-1，b-2と表記）と淀川河川水（YR）を採取した．淀川流域の一部の下水処理場にはオゾンによる前駆物質が流入し，放流水中にも存在していることが報告されている[22,23,27]．2011年3月，利根川流域の3下水処理場放流水（f～h下水処理場），事業所排水口直下の水路の水（i），利根川河川水（TR）を採取した．YR，TRのいずれも調査対象とした下水処理場，事業所排水口直下の水路の下流に，また，浄水場（D～H浄水場：利根川流域；N，O浄水場：淀川流域）の上流に位置している．これら淀川流域，利根川流域で採取した排水や河川水について，N-ニトロソアミン類濃度，クロラミン処理，オゾン処理による前駆物質について調査した．なお，淀川流域，利根川流域の下水処理場や事業所は，浄水場の上流に位置している．全ての試料の採取はスポット採取であり，また，プロセス水の採取では到達時間の考慮は行っていない．

(3) クロラミン処理，オゾン処理によるNDMAの生成

クロラミン処理，オゾン処理のいずれも反応容器には容量1 Lのガラス製のねじ口瓶を用いた。クロラミン処理によるN-ニトロソアミン類の生成は，試料量は600 mL，反応時間は24時間，pH 7（5 mMりん酸緩衝液），水温は20℃，24時間後のクロラミン濃度が3.0±0.5 mg/Lの条件で評価した[24,25]．本研究でのクロラミン処理条件では，処理前後でpHは特に変化しなかった．オゾン 処理によるN-ニトロソアミン類の生成は，半回分式で行った．高圧ガスによる純酸素を原料とし，オゾンガス発生器はPOX-20（富士電機）を用いた．試料量は800 mL，pH 7（5 mMりん酸緩衝液），水温は20℃，オゾンガス濃度は5 mg/L，オゾンガス流量は250 mL/分の条件とした．オゾン処理時間は，2～10分であった．オゾン処理条件の検討では，対象水のオゾンとの反応の進行の程度とNDMA生成との関連性の観点から，オゾン処理時間の影響を評価した．一方，他の運転パラメータであるオゾンガス濃度やオゾンガス流量は一定とした．これは，これら運転パラメータは，オゾンの液相から液相への移動速度に影響するが，対象水のオゾンとの反応の進行の程度

については，これらを一定にしても，基本的にオゾン処理時間を変えれば評価できると考えたためである．ただし，ばっ気による気散に対しては，オゾンガス濃度やオゾンガス流量は影響すると考えられるが，本研究では，その点の考慮はできていない．

(4) 測定方法

N-ニトロソアミン類濃度は，これまで著者らが報告してきたNDMAの場合[22),24),25)]と同様，固相抽出で試料の濃縮を行った後，UPLC-MS/MSを用いて測定した．まず，内部標準として用いた各*N*-ニトロソアミン類の同位体を試料に添加し，その後に濃縮を行った．表流水，下水処理水の場合，濃縮前にガラス繊維ろ紙（GF-F；Whatman）でろ過を行った．濃縮用カートリッジとしてAC-2（400 mg×2，Waters）を，精製用カートリッジとしてFlorisil（1 g，Waters）を用いた．濃縮手順は，既報のとおりである[22),24),25)]．UPLC（Acquity UPLC；Waters）は，分離カラムにAcquity UPLC BEH C18（1.7 mm×150 mm；Waters）を使用した。移動相は，0.1%ギ酸水溶液とアセトニトリルとし，アセトニトリルの割合が 20%（0 min）→ 20%（1 min）→ 90%（3 min）→ 90%（4.5 min）→ 95%（4.6 min）→ 95%（6 min）→ 20%（6.35 min）→ 20%（8.35 min）のグラディエント条件で，流量0.2 mL/minで送液した．試料注入量は30 μLとした．MS/MSは，Acquity TQDタンデム質量分析計（Waters）を用い，イオン化方法は電気化学イオン化法の正イオンモード（ESCI+）とした．多反応モニタリング（MRM）は，NDMAではm/z 74.9/43.1（定量用）と74.9/57.9（確認用）を，NDMA-d_6ではm/z 81.0/46.0を，NMorではm/z 117.0/87.0を，NMor-d_8ではm/z 125.0/95.0を，NPyrではm/z 100.97/55.0を，NPyr-d_8ではm/z 109.0/62.0を選定した．対象物質の定量下限値（LOQ）は，精製水を用いた添加回収試験で，相対回収率（内部標準の回収率で補正した値）の変動係数（CV）が10%以下であった最低の添加濃度とした．すなわち，NDMAとNMorのLOQは1.0 ng/L（n=6，NDMAの相対回収率の平均値は120%，NMorでは100%），NPyrのLOQは3.0 ng/L（n=4，相対回収率の平均値は120%）であった．このとき，それぞれの絶対回収率の平均値は，50%，62%，46%であった．また，河川水と水道水については，添加回収試験（添加濃度：10 ng/L）を行ったところ，NDMAの相対回収率は100%と110%，NMorでは99%と93%，NPyrでは110%と130%であった（CVは6%以下（n=2））．下水処理場放流水を用いた添加回収試験は行わなかったが，本研究の実態調査において，下水処理場放流水を対象とした場合，NDMA，NMor，NPyrの内部標準の絶対回収率の平均値は，それぞれ50%，64%，32%であった．

クロラミン濃度は，*N,N*-ジエチル-*p*-フェニレンジアミンと硫酸第一鉄アンモニウムを用いた滴定法により測定した[30)]．オゾンガス濃度はPG-620HA（荏原実業）によって，溶存オゾン濃度はインジゴを用いた吸光光度法によって測定した[30)]．全有機炭素（TOC）濃度はTOC計（TOC-V CPH；島津製作所）により，全窒素（TN）濃度はTOC計に接続したTN計（TNM-1；島津製作所）により測定した．硝酸態窒素および亜硝酸態窒素濃度はイオンクロマトグラフ（DX-500；ダイオネクス）を用いて測定した．アンモニア態窒素濃度はインドフェノール法[31)]により測定した．有機態窒素（TON）濃度は，TN濃度と硝酸態窒素，亜硝酸態窒素，アンモニア態窒素濃度との差とした．

3. 結果および考察

(1) 全国の浄水場におけるNDMA濃度とクロラミン処理の影響

表-1に，夏季，冬季における19浄水場の原水，浄水中の*N*-ニトロソアミン類の実態調査結果を示す．夏季において同一浄水場で2回調査を実施したり，冬季では実施していない浄水場があるため，対象浄水場数と試料数は一致していない．

原水の場合，NDMAは，夏季では20試料水中5試料水から検出され，その濃度範囲は1.1～2.0 ng/Lであった．冬季では16試料水中6試料水から検出され，その濃度範囲は1.2～3.8 ng/Lであった．冬季の方が，検出濃度の最大値が高い結果が得られたが，夏季に検出された地点で冬季には不検出となった場合もあり，今回の調査では冬季の方が濃度が高いとは判断できなかった．

表-1 浄水場での*N*-ニトロソアミン類濃度の調査結果

対象物質	原水		浄水	
	検出率*	濃度 (ng/L) **	検出率*	濃度 (ng/L) **
NDMA				
夏季	5/20	1.1～2.0	5/20	1.0～2.2
冬季	6/16	1.2～3.8	4/16	1.3～8.3
NMor				
夏季	0/20	–	2/20	1.1～1.3
冬季	4/16	1.2～4.2	2/16	1.1～3.3
NPyr				
夏季	0/20	–	0/20	–
冬季	0/16	–	0/16	–

*検出試料数/測定試料数，** 検出試料の濃度範囲

また，NDMAが検出された原水の多くは，淀川流域か利根川流域の浄水場で，最も濃度が高い試料も淀川流域の浄水場であった．すなわち，両流域の浄水場の原水中からは，NDMAが検出されやすく，これは過去の調査結果と一致していた[24]．また，原水中のNDMA濃度と一般水質項目との関連性は，認められなかった．

浄水中のNDMAについて見ると，夏季では20試料水中5試料水から検出され，その濃度範囲は1.0～2.2 ng/Lであった．冬季では16試料水中4試料水から検出され，その濃度範囲は1.3～8.3 ng/Lであった．原水の場合と同様に，冬季の方が濃度が高かった．特に，浄水中の濃度が8.3 ng/Lであった浄水場は，オゾン処理を導入している淀川流域のO浄水場であった．これは，同浄水場の原水には，オゾン処理によるNDMAの前駆物質が存在しているため，オゾン処理の結果，NDMA濃度が上昇したことによると考えられた（次節参照）[22,23,27]．

原水中のNMor濃度は，夏季では全ての試料で<1.0 ng/Lであったが，冬季では16試料水中4試料水から検出され，その濃度範囲は1.2～4.2 ng/Lであった．浄水中のNMor濃度は，夏季では20試料水中2試料水から検出され，その濃度範囲は1.1～1.3 ng/Lであった．冬季では16試料水中2試料水から検出され，その濃度範囲は1.1～3.3 ng/Lであった．これらの結果から，NMorは，NDMAよりは頻度は高くはないが，原水，浄水中に存在していること，NDMAの場合と同様に冬季に検出率が高くなる傾向があることがわかった．また，原水中と浄水中でNMor濃度を比較すると，増加している場合や減少している場合もあったが，ほとんど変わらない場合が多かったことから，浄水プロセスでNMorは除去されにくいことがわかった．NPyrについては，原水と浄水のいずれの試料からも検出されなかった．

次に，クロラミン処理による影響について検討した．図-1に，原水のクロラミン処理後のNDMA濃度を示す．クロラミン処理の影響について検討しなかったF浄水場は除いている．H，N浄水場は冬季の調査は行っていない．O浄水場では夏季の調査を2回実施し，それぞれ4.7，17 ng/Lであったためその平均11 ng/Lを記載した．

夏季，冬季で，それぞれ19試料中18試料，15試料中14試料からNDMAは検出され，1.0～17 ng/L，1.6～25 ng/Lの濃度範囲であった．また，今回の調査では，夏季よりも冬季において，クロラミン処理後のNDMA濃度が高い，すなわち，NDMA前駆物質が存在している傾向にあった．クロラミン処理後のNDMA濃度が，夏季，冬季のいずれかで5.0 ng/L以上であったのは9浄水場あり，その中に淀川流域あるいは利根川流域の6浄水場は全て含まれていた（D～H浄水場：利根川流域；N，O浄水場：淀川流域）．この結果は，著者ら[24]が2008年に実施した調査と

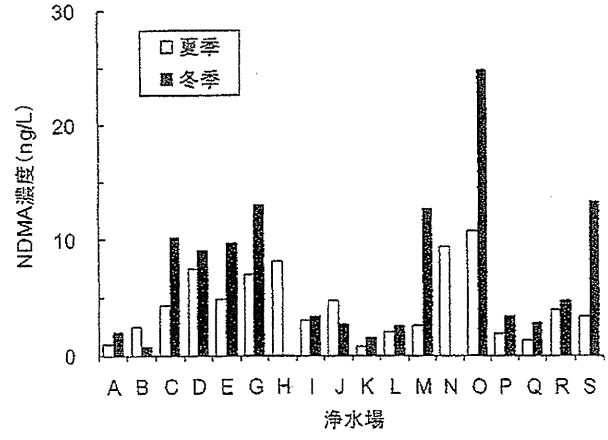

図-1　原水のクロラミン処理後のNDMA濃度（H，N浄水場は冬季の調査は未実施，夏季に2回調査したO浄水場は平均値を表示，図中<1.0 ng/Lの場合も値を表示）

同様の傾向であった．一方，淀川流域，利根川流域以外の3浄水場でもクロラミン処理後のNDMA濃度が比較的高かったが，この結果は，2008年に行った調査とは異なる傾向にあった[24]．この理由として，過去の報告の調査時期は夏季であり，本研究で，クロラミン処理後のNDMA濃度が比較的高かったのは冬季の結果であったためと考えられた．また，クロラミン処理後のNDMA濃度と一般水質項目との関連性は，認められなかった．NMorとNPyrの場合，いずれの試料でも，クロラミン処理後に濃度が増加する傾向はほとんど認められなかった．

(2) 高度浄水プロセスでのN-ニトロソアミン類の挙動

図-2に，オゾン処理を導入している5浄水場における，高度浄水プロセスでのNDMAの挙動について示す．G，O浄水場のみ夏季と冬季の両方で調査した．砂ろ過の設置地点が，凝集沈殿後，活性炭処理後と浄水場によって異なっていたため，図では省略した．また，活性炭処理後に，砂ろ過と塩素処理，あるいは塩素素処理を行っているため，活性炭処理水と浄水とは異なる水である．

淀川流域の浄水場（O，N浄水場）の場合，夏季の調査では，浄水プロセスでそれほど濃度は変わらなかった．冬季の調査では，N浄水場において，オゾン処理でNDMA濃度が増加し，後段の活性炭処理で濃度が低下するが，除去しきれずに浄水中でもNDMAが検出された．この挙動は，これまで報告されていた，冬季における淀川流域の高度浄水プロセスでの挙動と一致した[23]．一方，利根川流域の浄水場（F～H浄水場）の場合，夏季の調査では，浄水プロセスでそれほど濃度は変わらなかったが，そのうちのG浄水場の冬季の調査では，N浄水場ほどではないが，オゾン処理でNDMA濃度が増加した．ただし，その後，活性炭処理で濃度が低下した．これまで